Available online at www.sciencedirect.com
ScienceDirect
Ceramics International 33 (2007) 1149–1154
CERAMICS INTERNATIONAL
www.elsevier.com/locate/ceramint

Addition of Al–Ti–C master alloys and diopside to improve the performance of alumina matrix ceramic materials

Changxia Liu [a,b,*], Jianhua Zhang [a,*], Junlong Sun [a,b], Xihua Zhang [c], Yujing Hu [a]

[a] Department of Mechanical Engineering, Shandong University, Jinan 250061, Shandong Province, PR China
[b] Communications Institute, Ludong University, Yantai 264025, Shandong Province, PR China
[c] Department of Materials Science and Engineering, Shandong University, Jinan 250061, Shandong Province, PR China

Received 31 October 2005; received in revised form 7 February 2006; accepted 16 March 2006
Available online 10 July 2006

Abstract

In the present work, Al–Ti–C master alloys and diopside are introduced in alumina matrix ceramic materials. Composites are fabricated by the technology of transient liquid phase sintering, during which new phases such as $Al_6Si_2O_{13}$, AlN and $CaO{\cdot}6Al_2O_3$ are produced by the chemical reactions taking place among alumina and the additives. The densification rate of the composites as a function of Al–Ti–C volume content is discussed. The hardness, the fracture toughness and the bending strength of the composites are tested. Meanwhile, the effects of additives on mechanical properties and fracture mechanism of alumina matrix ceramic materials are analyzed and discussed together with the refining performances of Al–Ti–C master alloys.

Keywords: B. Composites; Alumina; Al–Ti–C master alloys; Toughening

1. Introduction

Alumina is a widely used ceramic material due to its refractoriness, wear resistance and chemical stability. However, the brittleness of pure alumina limits its potential applications. So how to improve the bending strength and fracture toughness of alumina matrix ceramic materials has been a key subject for many years and till now many interesting results have been obtained [1–8]. But in these studies, excellent mechanical properties are obtained always with a cost increase on account of the expensive second phases [9–13]. So low-cost has also been regarded as a priority when researchers were designing the composition of alumina matrix ceramic materials. Al–Ti–C master alloys just have the virtue of low-cost compared to other additives. The sources of α-Al_2O_3 are also in abundance in China and the price is low. Incorporation of Al–Ti–C master alloys into alumina matrix ceramic materials has been shown to result in significant improvement in fracture toughness [14]. So low-cost Al–Ti–C master alloys were chosen as the toughening phase in order to reduce the cost of alumina matrix ceramic materials. It has been reported in reference [15] that the smaller the sizes of particles are, the lower the temperature to sinter alumina will be. The refining performances of Al–Ti–C have been applied to Al and its alloys [16–18], and excellent effects have been achieved. But there are few articles from literature reporting about the refining performances of Al–Ti–C on alumina ceramic materials. Diopside ($MgCa(SiO_3)_2$) also has the virtue of low cost, and it acts as accessory ingredient during the process of transient liquid phase sintering.

In this paper, alumina matrix ceramic materials with the addition of Al–Ti–C master alloys and diopside are fabricated by the hot pressing technology. The cooperative toughening effect of Al–Ti–C master alloys and diopside on mechanical properties and microstructure of alumina matrix ceramic materials is discussed.

2. Experimental procedure

Commercial Al_2O_3 powder of high purity (99.99%) and small grain size (0.5–1 μm) was used as the starting materials. Al–Ti–C master alloys and diopside were used as additives. Al–Ti–C master alloys are developed by the department of

* Corresponding authors. Tel.: +86 531 82266727.
E-mail addresses: hester5371@gmail.com (C. Liu), jhzhang@sdu.edu.cn (J. Zhang).

0272-8842/$32.00
doi:10.1016/j.ceramint.2006.03.018

Table 1
Compositions of hot-pressed composites

Specimen	Compositions (vol.%)
A_0	100%Al_2O_3
A_7	87%Al_2O_3 + 6% diopside + 7%Al–Ti–C
A_{10}	84%Al_2O_3 + 6% diopside + 10%Al–Ti–C
A_{13}	81%Al_2O_3 + 6% diopside + 13%Al–Ti–C
A_{25}	75%Al_2O_3 + 6% diopside + 25%Al–Ti–C

materials science and engineering in Shandong University, the alloy used in present study has the composition Al–8%Ti–2%C. Diopside is composed of SiO_2 (55 wt.%), CaO (24 wt.%) and MgO (18 wt.%). The volume content of Al–Ti–C master alloys ranged from 7 to 25 vol.% is listed in Table 1. (The suffix in A_0, A_7, A_{10}, A_{13} and A_{25} represents the volume content of Al–Ti–C. For example, A_0 means the volume content of Al–Ti–C is zero.)

Firstly, the raw materials were blended with each other according to certain proportions and ball milled for 60 h in an alcohol medium to obtain a homogeneous mixture. Secondly, the slurry was dried in vacuum and screened. Thirdly, the mixed powders were pressed into disc compacts 21 mm in diameter and 5–7 mm in height. Last, hot-pressing was used to sinter the powder mixture in a graphite die under nitrogen protection. The specimens were heated up to 1450 °C (30 °C min^{-1}) with a pressure of 28 MPa for 30 min, except A_{13} for 45 min.

The sintered specimens were machined with a grinding machine. Standard test pieces (3 mm × 4 mm × 36 mm) were obtained through rough grinding, finish grinding with diamond wheels and polishing. Three-point-bending mode was used to measure the bending strength with a span of 20 mm and at a crosshead speed of 0.5 mm/min. Vickers hardness was measured on polished surface with a load of 9.8 N for 5 s with a micro-hardness tester (MH-6). Fracture toughness measurement was performed using indentation method with a hardness tester (Hv-120), and results were obtained by the formula proposed by Cook and Lawn [19].

XRD (D/max-2400) analysis was undertaken to identify the crystal phases present after sintering. Microstructural observations of fracture surfaces and the cracks were examined on polished surface by scanning electron microscopy (HITACHI S-570).

3. Results and discussion

3.1. X-ray diffraction phase analysis

The X-ray diffraction analyses of Al–Ti–C master alloys and A_7 are shown in Figs. 1 and 2 respectively. It is clear from Fig. 1 that Al–Ti–C master alloys are composed of Al and TiC phases, which is similar with the data reported by Jiang et al. [20]. Further, there exist in A_7 the $Al_6Si_2O_{13}$, AlN, Al_2O_3, $CaO{\cdot}6Al_2O_3$, CaO, SiO_2 and TiC phases. Theoretically there should exist MgO and Al in the composites, but XRD analysis does not show the occurrence of MgO and Al. This is because the volume fraction of diopside is only 6 wt.% in the composites, and that of MgO is 18 wt.% in diopside, so the percent of MgO in the composites is only 1.08 wt.%. The

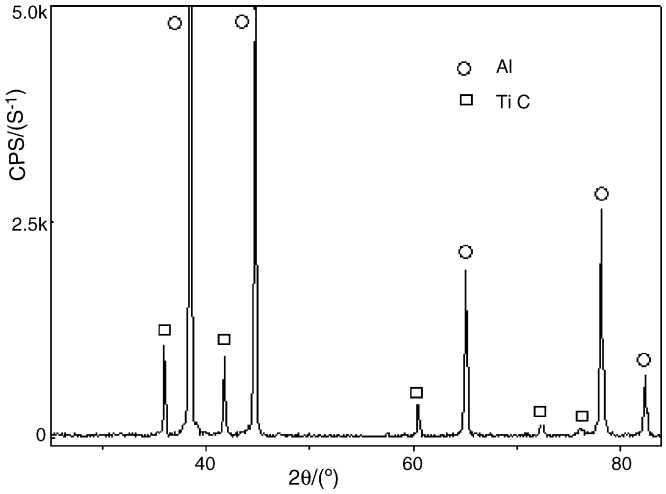

Fig. 1. X-ray diffraction phase analysis of Al–Ti–C master alloys.

amount of MgO is too small to be detected by XRD analysis. The sintering temperature is 1450 °C, which is much higher than the melting point of Al (660 °C). Hence Al is in the molten state and some part may have escaped during the sintering process, the other reacting with N_2 (the protection atmosphere) to form the new phase AlN:

$$2Al + N_2 \rightarrow 2AlN \quad (1)$$

Two following chemical reactions yielding mullite and $CaO{\cdot}6Al_2O_3$ may occur besides Eq. (1):

$$3Al_2O_3 + 2SiO_2 \rightarrow Al_6Si_2O_{13} \quad (2)$$

$$6Al_2O_3 + CaO \rightarrow CaO \cdot 6Al_2O_3 \quad (3)$$

Based on thermodynamics analysis of the reaction equation, we can get the following ranking:

$$\Delta G^{\theta}_{T_1} < 0, \quad \Delta G^{\theta}_{T_2} < 0 \quad \Delta G^{\theta}_{T_3} < 0$$

where, $\Delta G^{\theta}_{T_1}$, $\Delta G^{\theta}_{T_2}$ and $\Delta G^{\theta}_{T_3}$ represent the Gibbs free energy of the Eqs. (1)–(3), respectively. XRD analysis shows that AlN, $Al_6Si_2O_{13}$ and $CaO{\cdot}6Al_2O_3$ actually exist in specimen of A_7 as previously mentioned.

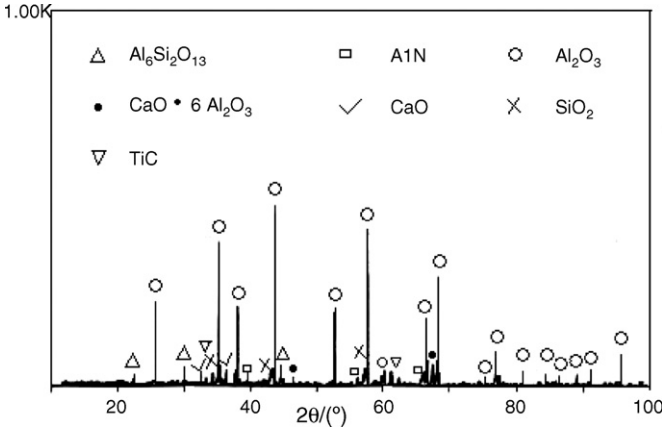

Fig. 2. X-ray diffraction phase analysis of A_7.

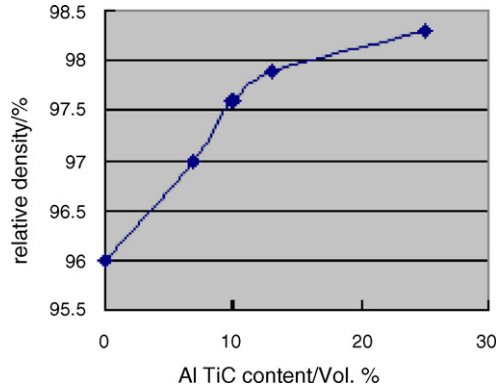

Fig. 3. Relation of Al–Ti–C content and relative density.

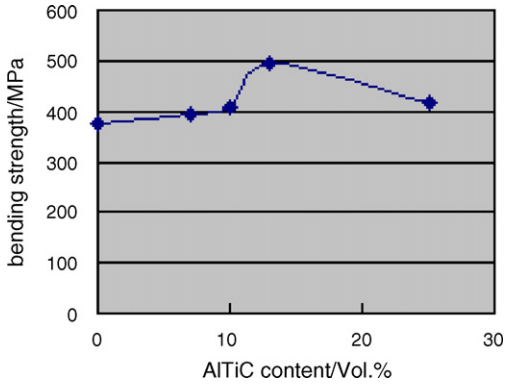

Fig. 5. Relation of Al–Ti–C content and bending strength.

3.2. Densification of the composites

Fig. 3 show the relations of Al–Ti–C volume content and relative density of the composites sintered at 1450 °C. It is clear from the figure that the relative density of A_0 is 96%, and the relative density of the composites increases sharply (up to ≈98%) as the addition amount of Al–Ti–C master alloys is raised from 0 to 13 vol.%. This trend becomes slowly with further addition of Al–Ti–C master alloys, and the relative density of A_{25} specimen is only 98.3%. Obviously, the densification rate of the composites increases with the volume content of Al–Ti–C master alloys increasing.

3.3. Mechanical properties

The relations of Al–Ti–C volume content and hardness, bending strength, fracture toughness of hot-pressed alumina matrix ceramic materials are shown in Figs. 4–6, respectively. The hardness and bending strength of pure alumina is respectively 16.7 GPa and 374 MPa, and the fracture toughness is 3.42 MPa $m^{1/2}$. The hardness of the composites increases as the Al–Ti–C content is raised from 0 to 10 vol.%, and then decreases from 10 to 25 vol.%. There are two factors influencing the hardness of composites, namely a hardness effect due to the addition of Al–Ti–C master alloys and a densification effect of the composites. The hardness of the composites increases for the reason that the densification effect is stronger than the hardness effect, otherwise the hardness of the composites will decrease. In the first stage (0–10 vol.% addition), the densification effect is dominant and the hardness is enhanced, while the hardness is reduced as the hardness effect is in turn becoming dominant (10–25 vol.% addition). The effects of Al–Ti–C master alloys and diopside on the bending strength and fracture toughness of the composites are similar. The bending strength and fracture toughness increase with the amount of Al–Ti–C master alloys increasing before 13 vol.%, then reach their maximum values for 13 vol.% and decrease after 13 vol.%.

Compared to the mechanical properties of pure alumina, significant improvements have been attained in hardness and fracture toughness, which reach their maximum values of 22.4 GPa and 6.07 MPa $m^{1/2}$ as the volume content of Al–Ti–C is 10%. The bending strength reaches its maximum value of 494 MPa when the volume content of Al–Ti–C is 13%. As a result, in virtue of the addition of Al–Ti–C master alloys and diopside, the hardness, bending strength and the fracture toughness of alumina matrix ceramic materials are enhanced by 34.1%, 29.4% and 77.5% with respect to pure alumina.

3.4. Analysis of microstructures

SEM photomicrographs of fracture surface of pure alumina are shown in Fig. 7, those of A_7, A_{10}, A_{13} and A_{25} are shown in

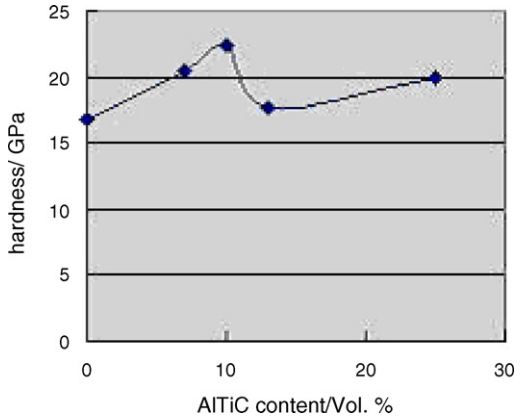

Fig. 4. Relation of Al–Ti–C content and hardness.

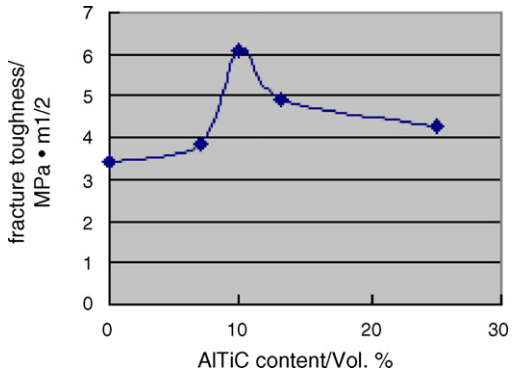

Fig. 6. Relation of Al–Ti–C content and fracture toughness.

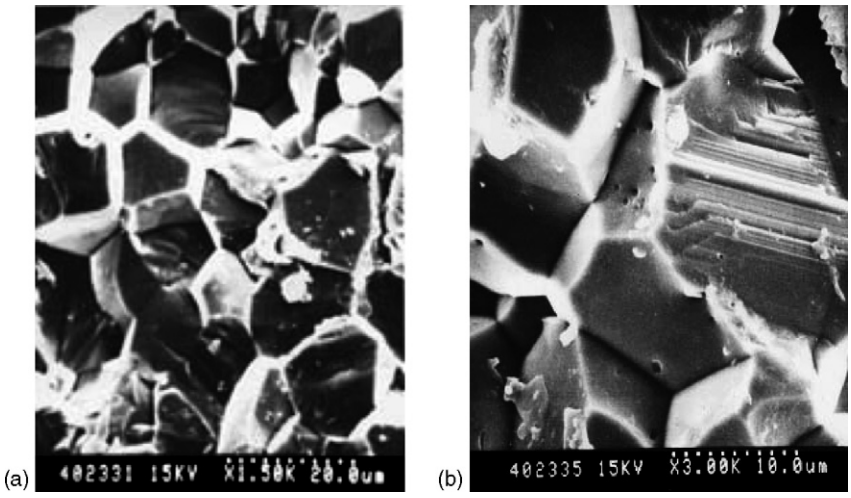

Fig. 7. SEM photomicrographs of pure alumina at different magnification.

Fig. 8. Composites hot pressed at 1450 °C show a homogeneous distribution of alumina grains and additive particles. As seen from Fig. 7(a), the fracture mode of pure alumina is mainly intergranular failure, although some of the larger alumina grains show transgranular failure. The fracture surface of pure alumina is quite smooth owing to the intergranular mode of fracture except a few brittle rupture (Fig. 7(b)), namely some particles break off by reason of the brittleness of alumina. Furthermore, there are a few tracks shaped by the drawingout of Al_2O_3 grains. On the contrary, the fracture surfaces of alumina matrix ceramic composites are relatively rough; moreover, the roughness of fracture surface increases with the increment of Al–Ti–C master alloys in the composites (Fig. 8(c and d)). The fracture mechanism changes from intergranular failure to a combination of intergranular failure and transgranular failure (Fig. 8(a and b)) and intergranular failure most likely results from the interfacial weakness. Transgranular failure becomes the main fracture mode as the addition amount of Al–Ti–C continues to increase (Fig. 8(c and d)). The fracture surface of composites is roughest for Al–Ti–C volume content up to 13%.

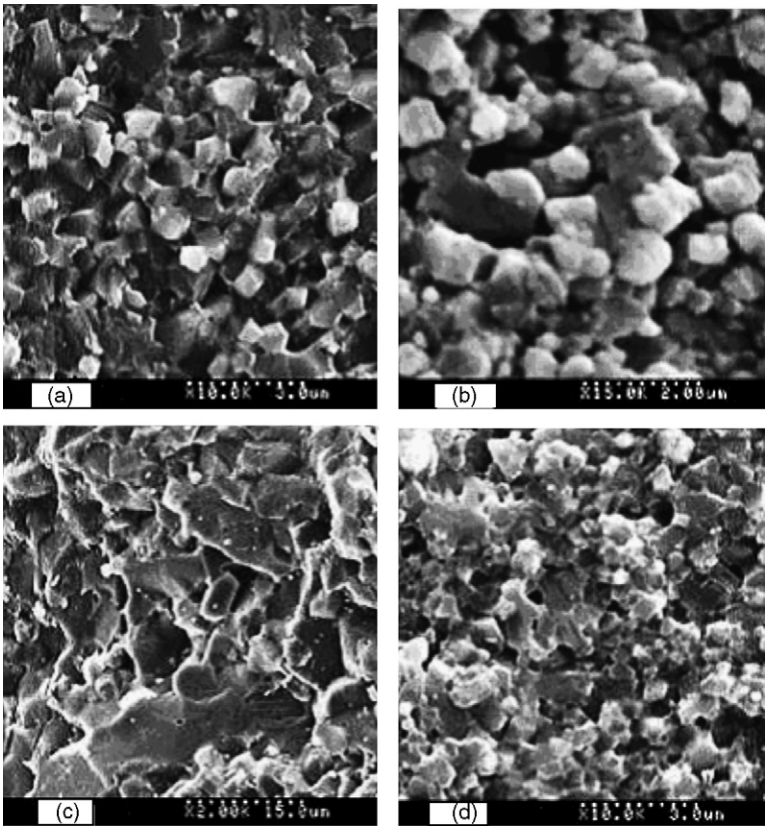

Fig. 8. SEM photomicrographs of the specimens: (a) A_7; (b) A_{10}; (c) A_{13}; (d) A_{25}.

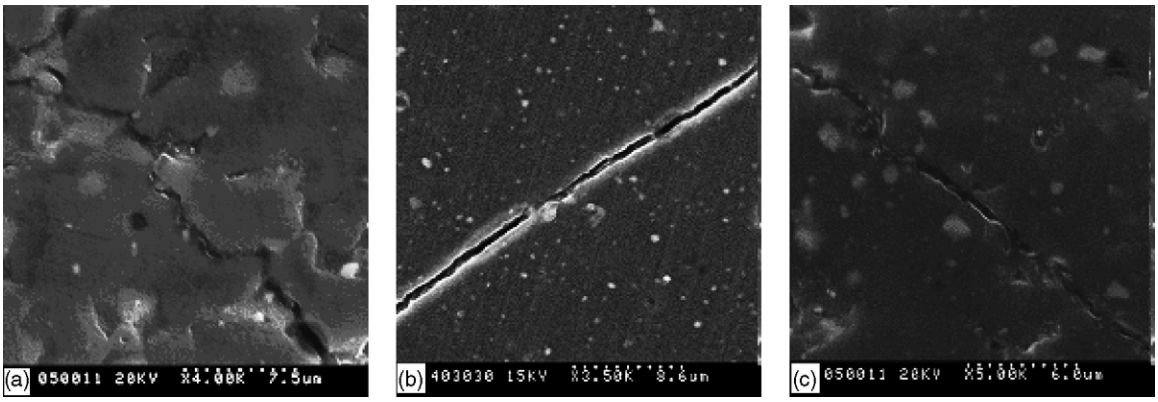

Fig. 9. SEM photomicrographs of indentations cracks in specimens: (a) A_{10}; (b) A_{13}; (c) A_{25}.

The addition of Al–Ti–C master alloys changes the fracture mechanism from intergranular failure to transgranular failure, which makes it clear that the bonding of grains become stronger. This change may enhance the bending strength of the composites but is of no use for the improvement of fracture toughness.

Fig. 9 shows crack propagation paths in A_{10}, A_{13} and A_{25}. Among these figures, deflection obviously occurred in Fig. 9(a), while the propagating cracks in Fig. 9(b and c) are direct. Intergranular failure is the main fracture mode in A_{10}, which results in the deflection. The cracks are forced to extend between the grains and more fracture energy is required to make the composites rupture. In consequence, fracture toughness of A_{10} is improved to a great extent. However, transgranular failure of A_{13} and A_{25} is the main factor for direct propagating crack, and their fracture toughness is lower.

3.5. Analysis of refining performances

The grain size of pure alumina is larger than that of the composites toughened by Al–Ti–C master alloys and diopside (Figs. 7 and 8). The grains of Al_2O_3 in composites may be restrained from abnormal growing owing to the addition of Al–Ti–C master alloys. The mean grain size is reduced dramatically to 0. 8 μm compared with a grain size of 12 μm in the pure alumina hot pressed under identical conditions, except that of A_{13} is 8 μm for the longer holding time of 45 min. The reason is as follows, on one hand, two Al and TiC phases exist in Al–Ti–C master alloys as shown in Fig. 1, the melting point of Al is 660 °C, so the liquid-phase sintering begins as the temperature goes above 700 °C. The reaction between Al and N_2 starts to occur on the surface of the disc compacts. However, the development of the reaction is slow owing to high chemical bond strength of Nitrogen molecule and it is difficult for N_2 to infiltrate through the compact AlN by reason of the very low dissolvability of N_2 in Al and strong compactness of AlN. So it takes long time to complete the transformation of Al to AlN [21]. On the other hand, during the sintering process, $TiAl_3$ may be produced by the following chemical reaction:

$$3TiC + 2Al_2O_3 + 5Al \rightarrow 3TiAl_3 + 3CO_2 \quad (4)$$

Simultaneously, based on thermodynamic analysis of the reaction equation, we can write the following expression:

$$\Delta G^{\theta}_{T_4} < 0 \quad (5)$$

where, $\Delta G^{\theta}_{T_4}$ represents Gibbs free energy of Eq. (4). $TiAl_3$ is a labile compound at the sintering temperature and then Ti is provided by the decomposition of $TiAl_3$. It has been reported that Ti has played a significant role in refining pure Al [22]. Furthermore, TiC has face centered cubic structure and it is a better nucleant for Al, so there is tendency for larger number of facets of the TiC particles to act as nucleating sites for Al particles [23]. For this good grain refining efficiency towards Al, there is abundant small size of Al grains surrounding alumina grains and thus prevent them from abnormal growing before Al reacts with N_2. At the end of the sintering process, Al is almost entirely transformed into AlN, which has a grains size of nanometer. These grains distribute evenly over alumina matrix ceramic materials and contribute to the refining effect [21].

4. Conclusion

The addition of Al–Ti–C master alloys obviously prompts the sintering of alumina matrix ceramic materials, the relative density of the composites reaches ≈98% as the volume content of Al–Ti–C master alloys is raised from 7% to 13%. Based on this good densification rate, improved mechanical properties have been attained. The hardness and fracture toughness reach their maximum values of 22.4 GPa and 6.07 MPa $m^{1/2}$ as the volume content of Al–Ti–C master alloys is 10%, while the bending strength reaches its maximum of 494 MPa as the volume content of Al–Ti–C is 13%. There are chemical reactions taking place among SiO_2, Al_2O_3, Al, N_2 and TiC in the process of sintering, and new phases namely, $Al_6Si_2O_{13}$, AlN, $CaO{\cdot}6Al_2O_3$ are produced. Composites hot pressed at 1450 °C show a homogeneous distribution of alumina grains and additive particles and the mean grain size was reduced to 0. 8 μm compared with a grain size of 12 μm in the pure alumina hot pressed under the same sintering conditions. A fracture mode changing from intergranular failure for pure alumina to transgranular failure for the composites is observed and may account for the slight increase in bending strength. The main cause is that the grain

boundaries of the composites are strengthened owing to the addition of Al–Ti–C master alloys and diopside.

Acknowledgements

The work described in this paper is supported by the Ministry of Education, PR China (no. 03101) and the Outstanding Young Scientist Rewards of Shandong Province, PR China (no. 03BS103).

References

[1] S.K.C. Pillai, B. Baron, M.J. Pomeroy, S. Hampshire, Effect of oxide dopants on densification, microstructure and mechanical properties of alumina–silicon carbide nanocomposite ceramics prepared by pressureless sintering, J. Eur. Ceram. Soc. 24 (2004) 3317–3326.

[2] D.H. Riu, Y.M. Kong, H.E. Kim, Effect of Cr_2O_3 addition on microstructural evolution and mechanical properties of Al_2O_3, J. Eur. Ceram. Soc. 20 (2000) 1475–1481.

[3] Y.Q. Fu, Y.W. Gu, H.J. Du, SiC whisker toughened Al_2O_3–(Ti,W)C ceramic matrix composites, Scripta Mater. 44 (2001) 111–116.

[4] V.M. Sglavo, F. Marino, B.R. Zhang, S. Gialanella, Ni_3Al intermetallic compound as second phase in Al_2O_3 ceramic composites, Mater. Sci. Eng. A 239–240 (1997) 665–671.

[5] W.H. Tuan, R.Z. Chen, T.C. Wang, C.H. Cheng, P.S. Kuo, Mechanical properties of Al_2O_3/ZrO_2 composites, J. Eur. Ceram. Soc. 22 (2002) 2827–2833.

[6] R.Z. Chen, W.H. Tuan, Toughening alumina with silver and zirconia inclusions, J. Eur. Ceram. Soc. 21 (16) (2001) 2887–2893.

[7] N.A. Travitzky, Microstructure and mechanical properties of alumina/copper composites fabricated by different infiltration techniques, Mater. Lett. 36 (1–4) (1998) 114–117.

[8] Y.G. Liu, D.C. Jia, Y. Zhou, Microstructure and mechanical properties of a lithium tantalate-dispersed-alumina ceramic composite, Ceram. Int. 28 (1) (2002) 111–114.

[9] S. Jiao, M.L. Jenkins, R.W. Davidge, Interfacial fracture energy-mechanical behavior relationship in Al_2O_3/SiC andAl_2O_3/TiN nanocomposites, Acta Mater. 45 (1) (1997) 149–156.

[10] S.I. Cha, K.T. Kim, K.H. Lee, C.B. Mo, S.H. Hong, Strengthening and toughening of carbon nanotube reinforced alumina nanocomposite fabricated by molecular level mixing process, Scripta Mater. 53 (7) (2005) 793–797.

[11] G. Vekinis, E. Sofianopoulos, W.J. Tomlinson, Alumina toughened with short nickel fibres, Acta Mater. 45 (11) (1997) 4651–4661.

[12] P.C. Ostertag, Influence of fiber and grain bridging on crack profiles in SiC fiber-reinforced alumina–matrix composites, Mater. Sci. Eng. A 260 (1–2) (1999) 124–131.

[13] N. Nawa, T. Sekino, K. Niihara, Fabrication and mechanical behaviour of Al_2O_3/Mo nanocomposites, J. Mater. Sci. 29 (1994) 3185–3192.

[14] X.H. Zhang, C.X. Liu, J.H. Zhang, Preparation of alumina matrix ceramic composite materials by the hot-press sintering process, J. Chin. Ceram. Soc. 33 (7) (2005) 14–18 (in Chinese).

[15] A. Nakajima, G.L. Messing, Liquid-phase sintering of alumina coated with magnesium aluminosilicate glass, J. Am. Ceram. Soc. 79 (12) (1996) 3199–3210.

[16] X.F. Liu, Z.Q. Wang, Z.G. Zhang, X.F. Bian, The relationship between microstructures and refining performances of Al–Ti–C master alloys, Mater. Sci. Eng. A 332 (1–2) (2002) 70–74.

[17] Z.Q. Zhang, X.F. Liu, X.F. Bian, Z.G. Zhang, Y. Wang, Microstructure and its influence on refining performance of AlTiC master alloys, Mater. Sci. Technol. 19 (2003) 1709–1714.

[18] M. Vandyoussefi, J. Worth, A.L. Greer, Effect of instability of TiC particles on grain refinement of Al and Al–Mg alloys by addition of Al–Ti–C inoculants, Mater. Sci. Technol. 16 (10) (2000) 1121–1128.

[19] R.F. Cook, B.R. Lawn, A modified indentation toughness technique, J. Am. Ceram. Soc. 66 (11) (1983) 200–201.

[20] Q.C. Jiang, H.Y. Wang, Y.G. Zhao, X.L. Li, Solid-state reaction behavior of Al–Ti–C powder mixture compacts, Mater. Res. Bull. 40 (2005) 521–527.

[21] K.F. Cai, C.W. Nan, R.Z. Yuan, Perparation and microstructure analysis of Al_2O_3–AlN–TiC composite ceramic, J. Chin. Ceram. Soc. 23 (4) (1995) 430–433 (in Chinese).

[22] Z.Q. Wang, X.F. Liu, X.F. Bian, Phases and refinement performances of AlTiC master alloys, Foundry 50 (6) (2001) 316–320 (in Chinese).

[23] G.S.V. Kumar, B.S. Murty, M. Chakraborty, Development of Al–Ti–C grain refiners and study of their grain refining efficiency on Al and Al–7Si alloy, J. Alloys Compd. 396 (2005) 143–150.